

Selective Hydrogenation of 1,3-Butadiene over a Pd/Cu(111) Single Atom Alloy Surface

Published as part of *The Journal of Physical Chemistry C special issue "Spectroscopic Techniques for Renewable Energy"*.

Mohammad Rahat Hossain and Michael Trenary*



Cite This: *J. Phys. Chem. C* 2024, 128, 19204–19209



Read Online

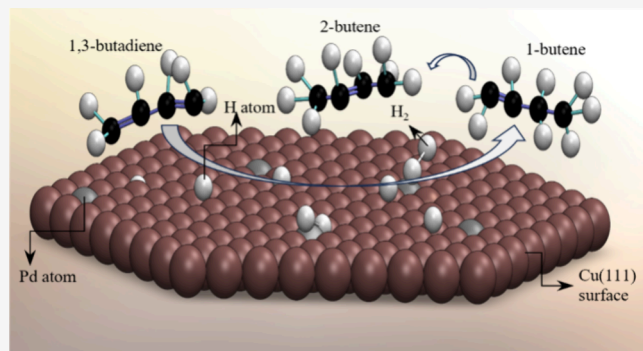
ACCESS |

Metrics & More

Article Recommendations

Supporting Information

ABSTRACT: The hydrogenation of 1,3-butadiene (BD, C_4H_6) to 1-butene (C_4H_8) over a Pd/Cu(111) single-atom alloy (SAA) was studied under ambient pressure conditions with reflection absorption infrared spectroscopy (RAIRS). The gas-phase reactants and products were monitored with RAIRS using *s*-polarized light, while *p*-polarization was used to search for adsorbed species present during the reaction. The formation of gas-phase 1-butene was revealed by the growth of a distinct infrared peak at 2878 cm^{-1} , whereas the consumption of gas-phase BD was measured by the decrease of a peak at 1587 cm^{-1} . The reaction rate was found to be first-order (1.12 ± 0.04) with respect to H_2 and zero-order (-0.12 ± 0.01) with respect to BD and corresponded to a turnover frequency of 36 s^{-1} at 380 K . From the temperature dependence of the rate constant, an activation energy of $63 \pm 3\text{ kJ/mol}$ was obtained. Complete conversion of 1,3-butadiene was observed with a high selectivity of 84% toward 1-butene without any production of butane. No surface species were detected with RAIRS during the reaction. Post-reaction analysis with Auger electron spectroscopy revealed carbon deposition, indicating that some dissociation accompanied hydrogenation.



1. INTRODUCTION

The hydrogenation of polyunsaturated hydrocarbons to selectively produce alkenes—a process vital for the petrochemical and polymer industries—has been a subject of considerable interest since the 1960s with the surge in olefin production from steam cracking.¹ While widely used in the refining and petrochemical sectors, establishing the surface mechanisms of selective hydrogenation of unsaturated compounds, including the conversion of 1,3-butadiene (BD) to 1-butene, remains crucial.² This hydrogenation reaction serves as a model to investigate catalyst properties, prompting ongoing research to understand catalyst performance, selectivity, and mechanisms in both fundamental and applied contexts.³

Traditional catalysts, such as Pd or Pt, are effective hydrogenation catalysts but are susceptible to coking. Single-atom alloy (SAA) catalysts offer a promising alternative.⁴ These catalysts leverage facile H_2 dissociation on active sites, typically isolated platinum or palladium atoms, combined with the selectivity of the transition metal host, such as copper, to improve both the selectivity and lifespan of the catalyst. Luccia et al. investigated the hydrogenation of butadiene to butenes on Pt/Cu(111) alloy surfaces in ultrahigh vacuum (UHV),

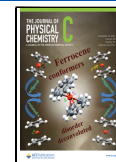
highlighting that individual Pt atoms on Cu(111) ensure stable activity with higher selectivity.⁵ Extending these findings to realistic pressures (1 bar), Pt/Cu single-atom alloy (SAA) nanoparticle catalysts were synthesized and tested, demonstrating that isolated Pt atoms activate H_2 dissociation and spillover of H atoms to Cu, leading to highly selective hydrogenation without decomposition or poisoning.⁵ Previous studies suggested that Pd(111) shows better selective control in hydrogenating 1,3-butadiene to 1-butene than Pt(111).^{6–9} This implies that isolated Pd atoms on a Cu host surface could be a promising model for this reaction, particularly for selectivity toward 1-butene among butenes. Lianos et al. found that $Pd_{50}Cu_{50}$ bimetallic alloys maintain selectivity to butenes with enhanced activity, attributed to a positive electronic ligand influence from surrounding Cu atoms. $Pd_{50}Cu_{50}(111)$ exhibits eight times higher activity than

Received: August 28, 2024

Revised: October 6, 2024

Accepted: October 22, 2024

Published: November 1, 2024



$\text{Pd}_{50}\text{Cu}_{50}(110)$, possibly due to a PdCu_3 ordered phase.¹⁰ Cooper et al. found that adding copper to Pd nanoparticles on graphite (PdCuG) improves 1,3-butadiene hydrogenation selectivity and reduces deactivation rates by limiting carbon deposits.¹¹ The PdCuG catalyst shows altered 1-butene selectivity, suggesting changes in hydrogen availability through electronic or geometric effects. In Pd–Cu catalysts, carbonaceous deposits crucially impact catalytic selectivities, overshadowing Cu promotion effects during butadiene-rich hydrogenation.¹¹

Here, we report the hydrogenation of 1,3-butadiene on a Pd/Cu(111) SAA catalyst with a Pd coverage of 0.027 monolayer (ML) under ambient pressure conditions. In a previous study, we used reflection absorption infrared spectroscopy (RAIRS) of CO to characterize the Pd/Cu(111) surface and found that at a Pd coverage of 0.03 ML, Pd exists as isolated atoms.¹² Using low-temperature STM, Marcinkowski et al. found that Pd is present as isolated atoms for Pd coverages of less than 0.1 ML.¹³ They also showed that Pd is concentrated near the ascending step edges to form Pd-rich brims rather than being uniformly distributed on the Cu(111) surface. This study of 1,3-butadiene hydrogenation follows our earlier work on the selective hydrogenation of acetylene and propyne over a Pd/Cu(111) SAA.^{14,15} The kinetics of this reaction were measured from the time dependence of the reactant and product concentrations through their gas-phase IR absorption peaks.

2. EXPERIMENTAL SECTION

The experiments were performed within a dual-stainless-steel chamber ultrahigh vacuum (UHV) system, as previously described in detail.^{16,17} The Cu(111) single crystal (99.9999% purity) with a diameter of 15 mm and a thickness of 2.5 mm (Surface Preparation Laboratory) was mounted and cleaned as described previously.¹⁸ Pd was deposited by heating a Pd wire wrapped around a W wire as described elsewhere.¹² Pd coverages were quantified with Auger spectra obtained with a beam energy of 2500 eV.

The fragmentation patterns of 1,3-butadiene and butene were obtained with a quadrupole mass spectrometer (QMS) at 1.1×10^{-7} Torr (Figure S1). The cracking pattern of butane was obtained from the NIST library.¹⁹ Analysis of the product gas with the QMS was conducted by transferring 1.1×10^{-7} Torr from the ambient pressure IR cell to the analysis chamber through a leak valve after completion of the reaction.

The RAIRS experiments used a Bruker Vertex 70v FTIR instrument and mercury cadmium telluride (MCT) detector. All RAIRS results are presented as absorbance spectra, and they were obtained with 1024 scans and a resolution of 4 cm^{-1} . A rotatable polarizer was used to obtain either *s*-polarized spectra (labeled *s*-Absorbance), which detect only gas-phase species, or *p*-polarized spectra, which detect both gas-phase and surface species. Subtraction of *s*-polarized spectra from the corresponding *p*-polarized spectra yields spectra sensitive to only surface species. Absorbance was used instead of reflectance or transmittance to quantify the partial pressures of gas-phase species from the peak intensities.

To calibrate our system's IR intensity versus pressure relationship, we measured spectra as a function of pressure in 0.1 Torr increments up to 1.0 Torr of 1,3-butadiene and 1-butene (Figures S2 and S3). The volume of the IR cell of $0.631 \pm 0.007 \text{ L}$ was determined from the ideal gas law by the expansion of argon at a known initial pressure and volume. 1,3-

Butadiene ($\geq 99.9\%$) and 1-butene ($\geq 99.9\%$) were purchased from Millipore Sigma and used without further purification.

3. RESULTS

Figure 1a shows *s*-polarized spectra taken over a period of 2 h after admitting 0.1 Torr of 1,3-butadiene and then 10 Torr of

Figure 1 consists of two panels, (a) and (b), showing gas-phase RAIRS spectra. Panel (a) is for a Cu(111) surface at 380 K, and panel (b) is for a 2.70% Pd/Cu(111) surface at 380 K. Both panels show absorbance spectra from 900 to 3200 cm⁻¹. The spectra are stacked vertically, with the bottom spectrum being the initial state and the top spectrum being the state after 36 minutes. The x-axis is labeled 'Wavenumber (cm⁻¹)' and the y-axis is labeled 's-Absorbance (a.u.)'. Peak assignments are provided for both panels. In panel (a), peaks are labeled at 907, 1013, 1137, 1387, 1458, 1597, 1605, 1619, 1638, 2973, 3001, 3033, 3064, and 3108 cm⁻¹. In panel (b), peaks are labeled at 912, 962, 1000, 1458, 1599, 2861, 2878, 2940, 2950, 2972, 3040, and 3066 cm⁻¹.

Figure 1. (a) Gas-phase RAIRS spectra taken after 0.1 Torr of 1,3-butadiene and then 10 Torr of H_2 were added to the IR cell containing a Cu(111) surface at 380 K. The spectra were taken over a reaction time of 36 min at 4 min intervals with the last scan taken after 2 h. (b) Gas-phase RAIRS spectra taken after 0.1 Torr of 1,3-butadiene and then 10 Torr of H_2 were added to the IR cell containing a 2.7% Pd/Cu(111) surface at 380 K shown over a reaction time of 36 min at 4 min intervals.

H_2 to the IR cell containing a clean Cu(111) surface at 380 K. All peaks correspond to those expected for the *s-trans* conformer of gas-phase BD.^{20,21} This conformer is planar and belongs to the C_{2h} point group. The IR active modes are of A_u (out of plane motion) and B_u (in plane motion) symmetry. In the gas-phase spectra in Figure 1, rotational side bands are evident, which complicates the appearance of the spectra, but the assignments are straightforward and follow those of De Maré et al.²¹ The peaks in the range of 2973–3108 cm^{-1} are due to $\nu(\text{C}=\text{H})$ and $\nu(\text{C}=\text{H}_2)$ stretching vibrations of B_u symmetry, while the peaks at 1596, 1380, 1013, and 907 cm^{-1}

19205

<https://doi.org/10.1021/acs.jpcc.4c05807>
J. Phys. Chem. C 2024, 128, 19204–19209

are assigned to $\nu(\text{C}=\text{C})$ asymm stretch (B_{u}), $\delta(\text{CH}_2)$ scissors (B_{u}), $\chi(\text{C}-\text{H})$ wag (A_{u}), and $\chi(\text{CH}_2)$ wag (A_{u}) modes, respectively. The vibrational transition near 1820 cm^{-1} is likely a $\nu_8(\text{A}_{\text{g}}) + \nu_{23}(\text{B}_{\text{u}})$ combination band where the fundamentals occur at 888 and 990 cm^{-1} . The lack of any intensity change with time in the spectra in Figure 1a demonstrates that there is no reaction between BD and H_2 over the clean $\text{Cu}(111)$ surface.

Spectra under the same conditions but over a $\text{Cu}(111)$ surface with a Pd coverage of 2.7% display distinctly different behavior, as shown in Figure 1b. The characteristic peaks of BD at, for example, 907 and $\sim 1600\text{ cm}^{-1}$, gradually disappear with time, and new peaks grow at, for example, 912 and 1458 cm^{-1} . The C–H stretch region also shows distinct changes with time. As the C–H stretch frequency depends on the hybridization at the carbon atom, the loss of intensity in the region above 3000 cm^{-1} and gain of intensity at or below 2900 cm^{-1} is a clear manifestation of the replacement of sp^2 carbon with sp^3 carbon. From our own measurements of the IR spectrum of gas-phase 1-butene (Figure S2), we assigned the new bands that grew at 2972 , 2900 , and 2878 cm^{-1} to 1-butene. In Figure S4, we make a direct comparison of the gas-phase spectra of 1,3-butadiene, 1-butene, and the product gas that forms above the 2.7% Pd/Cu(111) surface, which shows peaks that cannot be assigned to either 1,3-butadiene or 1-butene. We assign these peaks at 3040 , 2950 , 2940 , 2861 , and 962 cm^{-1} to 2-butene based on reference spectra of *trans*- and *cis*-2-butene.²² From the quantitative measurements described below, we conclude that there is 100% conversion of 1,3-butadiene, with the butene product consisting mainly of 1-butene. 1-Butene must form through 1,2-hydrogen addition, whereas 2-butene forms through 1,4-hydrogen addition. The weaker peaks associated with 2-butene implies that 1,4-hydrogen addition is less favorable, which may be related to one $\text{C}=\text{C}$ bond being closer to the surface, leading to 1,2-hydrogen addition to form 1-butene, with hydrogen addition to the second $\text{C}=\text{C}$ bond being less probable. As the IR spectra of *trans*- and *cis*-2-butene are not identical, in principle, it should be possible to identify which is formed. The intensity observed at 962 cm^{-1} in Figure S4 suggests that the product is *trans*-2-butene as there is a prominent peak near 960 cm^{-1} present in the IR spectrum of *trans*- but not for *cis*-2-butene.²² In the course of the reaction, the total pressure decreased from its initial value of 10.10 to 9.20 – 10.00 Torr, as expected for 100% conversion. Besides hydrogenation reactions, there is also some decomposition to deposit carbon on the surface, as revealed by the Auger electron spectroscopy results in Figure S5. This decomposition channel accounts for the decrease in total pressure by more than what was expected for stoichiometric hydrogenation to butene.

A comparison of the mass spectra of BD, 1-butene, and the product gas is shown in Figure S1. The product gas contains mainly unreacted H_2 , but the rest of the spectrum closely resembles that of 1-butene. For example, the largest peak in the product spectrum occurs at 15 amu, as is the case for 1-butene. In contrast, the largest fragment peak for BD occurs at 27 . The second and third largest peaks for 1-butene and the product gas occur at 27 and 41 amu, respectively, although the relative intensities of these peaks are slightly different in the two spectra. Based on a standard reference mass spectrum for butane,¹⁹ there is no evidence for butane in Figure S1 as its mass spectrum is dominated by a fragment at 43 amu, while there is negligible intensity at 43 amu for the product gas.

The IR spectra in Figure 1 were used to quantify the reactant and product concentrations in the IR cell based on the 1587 and 2878 cm^{-1} peaks for 1,3-butadiene and 1-butene, respectively. The partial pressures of BD and 1-butene during the reaction were derived from IR peak intensities by using calibration measurements of the IR intensities versus pressure (Figures S2 and S3). From the size of the IR cell and the ideal gas law, the number of moles of each was then determined. Figure 2 shows plots of the amounts of BD and 1-butene over a

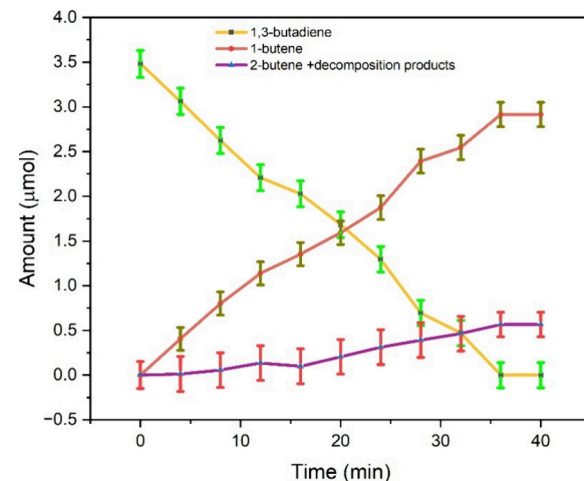


Figure 2. Amounts (in μmol) of 1,3-butadiene (yellow) and 1-butene (orange) versus time over a 2.7% Pd/Cu(111) surface at 380 K . Quantification was based on calibration measurements (Supporting Information) of the areas of peaks at 1587 and 2878 cm^{-1} versus pressure for 1,3-butadiene and 1-butene, respectively. The peaks were deconvoluted by Origin 2023 software. Assuming complete conversion of 1,3-butadiene, the remaining products, 2-butene and carbonaceous species from decomposition, are denoted in purple.

reaction time of 40 min . The results show that BD steadily falls from about $3.5\text{ }\mu\text{mol}$ to zero, while the amount of 1-butene rises from zero to reach a final value of about $2.9\text{ }\mu\text{mol}$, implying 84% conversion. The difference between the amount of BD consumed and the amount of 1-butene formed is attributed to the formation of 2-butene and decomposition products.

The kinetics of the reaction were studied by varying the quantity of either BD or H_2 while keeping the other reactant amount constant to determine the reaction orders. The quantities used are given in Table S1. Figure 3a shows \ln versus \ln plots of the initial reaction rate versus the amount of BD, keeping the amount of H_2 constant at $348\text{ }\mu\text{mol}$. For Figure 3b, the amount of BD was kept constant at $3.48\text{ }\mu\text{mol}$, and the amount of H_2 varied. From the slopes of the plots, we conclude that the reaction orders are -0.12 ± 0.01 for 1,3-butadiene and 1.12 ± 0.04 for hydrogen, respectively. These values imply that the reaction is essentially zero-order in BD and first-order in H_2 .

The rate of BD consumption can be used to calculate the turnover frequency (TOF), the reaction rate per active surface atom. From the size of the $\text{Cu}(111)$ crystal and the Pd coverage, we calculated a TOF of 36 s^{-1} , assuming that the reaction occurs solely at Pd sites. Alternatively, assuming that all surface atoms are active for hydrogenation yields a TOF of 0.97 s^{-1} . Since hydrogen spillover from Pd to Cu sites is known to occur,²³ the coverage of H atoms should be higher than the

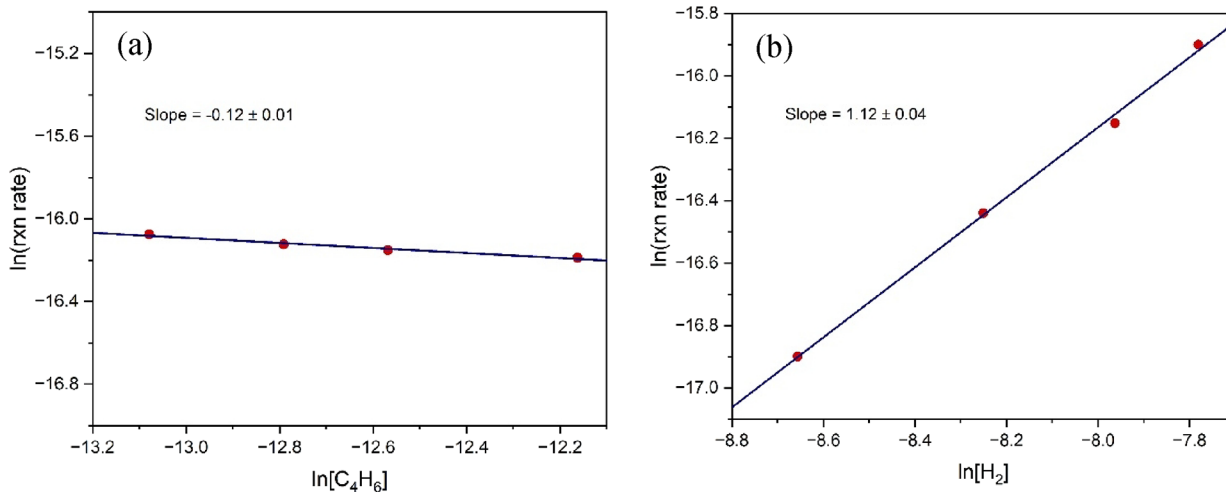


Figure 3. Linear fits to $\ln(\text{reaction rate})$ vs (a) $\ln [\text{C}_4\text{H}_6]$ and (b) $\ln [\text{H}_2]$ plots. The slopes of plots (a) and (b) give reaction orders in 1,3-butadiene and hydrogen, respectively.

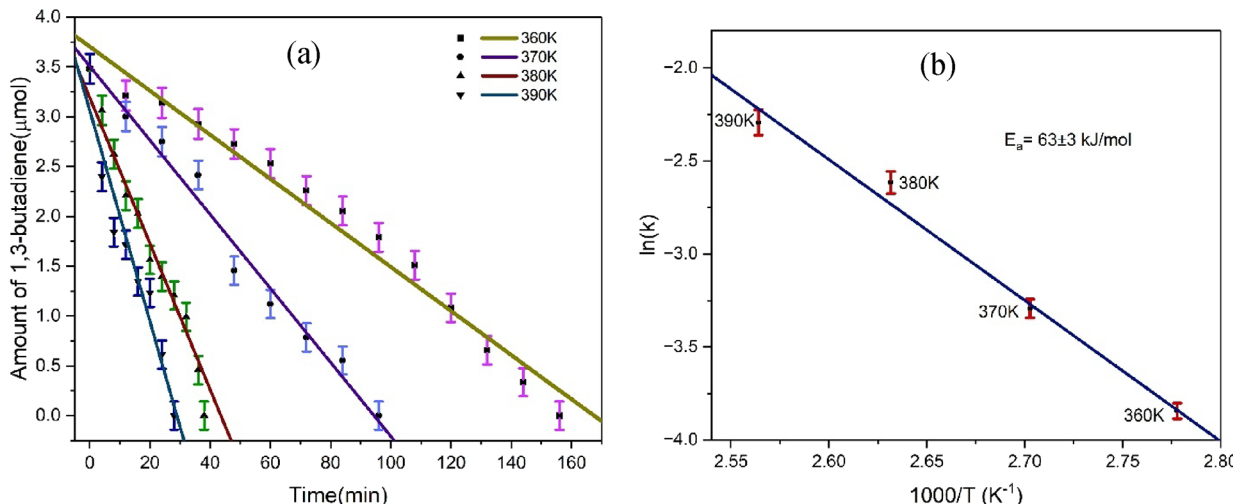


Figure 4. (a) Amount of 1,3-butadiene versus time at the indicated temperatures and linear fits to the data. The slopes of the lines give the zero-order rate constants. (b) Arrhenius plot of the temperature-dependent rate constants obtained from panel (a), which yields a slope corresponding to an activation barrier of $63 \pm 3 \text{ kJ/mol}$.

Pd coverage and, assuming that BD can react with H atoms at Cu sites, the TOF should fall between the values of 36 and 0.97 s^{-1} . These values are slightly lower than those for butadiene hydrogenation over Pd surfaces at 373 K (TOFs $\sim 38\text{--}180 \text{ s}^{-1}$).²⁴

We measured the temperature dependence of the kinetics of BD hydrogenation to obtain the activation energy of the reaction. Figure 4a shows a plot of the amount of BD versus time for temperatures of 360, 370, 380, and 390 K. As expected for a zero-order reaction, the amount decreases approximately linearly with time, with the slope of the lines giving the zero-order rate constant, k . At the lowest temperature studied, 360 K, some curvature of the data points is evident, indicating some deviation from zero-order kinetics. Figure 4b shows an Arrhenius plot of $\ln(k)$ versus $1/T$, which yields a straight line with the slope indicating an activation energy of $63 \pm 3 \text{ kJ/mol}$. Within the uncertainty, this falls in the range of the activation energies of 56–70 kJ/mol for BD hydrogenation over Pd catalysts.²⁵ The agreement indicates that the Pd atoms of the Pd/Cu(111) SAA have the same activity as the pure Pd catalysts. In contrast, the activation energies obtained over

Pd(110) and Pd(111) model catalysts were 36 and 25 kJ/mol, respectively.²⁴

4. DISCUSSION

In previous studies, we have used polarization-dependent RAIRS to identify surface species present during reaction under ambient conditions by subtracting *s*-polarized spectra from the corresponding *p*-polarized spectra.^{14–16} For this study of BD hydrogenation, no spectral features attributable to surface species were observed, even as the *s*-polarized spectra in Figure 1b reveal the hydrogenation of BD over the Pd/Cu(111) surface. Similarly, in polarization modulation RAIRS studies of BD hydrogenation over Pt₃Sn(111) and Pt(111)²⁶ and over Pd(111)²⁷ surfaces, no surface species were detected even as gas-phase spectra demonstrated that the hydrogenation reaction was occurring. This indicates either that the active intermediate was consumed as soon as it was formed so that its coverage never reached a high enough level to yield observable peaks or that all the vibrational modes of the intermediate had intrinsically weak transitions, making them unobservable even if the coverage of the intermediate was high. We have obtained

RAIRS and TPRS studies of BD on Cu(111) under UHV conditions and observed strong distinct RAIRS signals for both multilayer and monolayer BD, which TPRS showed have peak desorption temperatures below 130 and above 200 K, respectively. These low-temperature UHV studies demonstrate that adsorbed BD is detectable by RAIRS, so the lack of any spectral features during the reaction above 300 K is likely due to low coverage of the form of adsorbed BD that undergoes hydrogenation at temperatures above around 350 K.

In a study similar to ours, Silvestre-Albero et al. observed that 1,3-butadiene is rapidly hydrogenated to form three primary butenes (1-butene, *trans*-2-butene, and *cis*-2-butene) over Pd(111).^{24,27} They reported 75% conversion on Pd(111) at 373 K and 80% conversion on Pd(110) at 373 K, with lower selectivity for 1-butene (34% for Pd(111) and 14% for Pd(110)) than in our study. Silvestre-Albero et al. detected all products at the end of the reaction, which exhibited selectivity values toward butane of 8.4% for Pd(111) and 11.8% for Pd(110), with the remaining products consisting of *cis*- and *trans*-2-butene. They found that 1-butene, the thermodynamically less stable product, becomes the main product early in the reaction. Additionally, butane formed later from subsequent hydrogenation of adsorbed and/or readsorbed butenes. However, in our investigation, distinct vibrational modes specific to butane, such as at 2966 cm⁻¹, were not clearly detected. We therefore conclude that the Pd/Cu(111) SAA produces no butane. This is likely due to the low adsorption energy of 1-butene on Pd/Cu(111) so that it desorbs before it can be further hydrogenated to butane.

Another significant difference between our results and those of Silvestre-Albero et al. is the mechanism for formation of the 2-butenes (*cis* and *trans*).²⁴ In their case, as in ours, initially, the 1-butene concentration rose as the BD concentration fell. But unlike in our case, their 1-butene concentration reached a maximum with time and then fell to zero as concentrations of the 2-butenes and butane increased. They concluded that once adsorbed BD was hydrogenated, 1-butene could readsorb to undergo both hydrogenation and isomerization reactions. These mechanistic conclusions were supported by separately studying the hydrogenation of 1-butene. In contrast, our results in Figure 2 show that 1-butene and 2-butene grow together, suggesting parallel reaction pathways in which both 1,2- and 1,4-hydrogen addition to adsorbed BD can occur. A crucial observation by Silvestre-Albero et al. was that 1-butene isomerization required hydrogen. They therefore concluded that the same surface intermediate, a butyl species, was involved in the hydrogenation and isomerization. For the former, a second H atom was added to butyl to form butane, whereas a β -hydride elimination step led to 2-butene. Our results indicate that BD can be hydrogenated directly to 2-butene without first forming a butyl intermediate. We further speculate that this may be due to the presence of two forms of adsorbed BD on the Pd/Cu(111) surface, one of which favors 1,2-hydrogen addition and the other 1,4-hydrogen addition. To confirm this, more information is needed about the structure of BD on the Cu(111) and Pd/Cu(111) surfaces. We are currently addressing this issue through BD adsorption studies at low temperatures under UHV conditions.

5. CONCLUSIONS

We found that a 2.7% Pd/Cu(111) single-atom alloy (SAA) selectively hydrogenates 1,3-butadiene to butene with high activity. In the presence of 0.1 Torr of BD and 10 Torr of H₂,

the Pd/Cu(111) SAA exhibited an 84% selectivity toward 1-butene at 380 K, with the remaining product being both 2-butene and a carbonaceous deposit. The reaction was found to have an activation energy of 63 ± 3 kJ/mol and reaction orders of -0.12 ± 0.01 and 1.12 ± 0.04 with respect to 1,3-butadiene and H₂, respectively. The calculated turnover frequency (TOF) at the Pd sites was 36 s^{-1} at 380 K. These parameters derived from the kinetics of the reaction are similar to those obtained for pure Pd catalysts, demonstrating that an SAA achieves the high activity of a precious metal such as Pd in the most efficient way possible while also achieving a high degree of selectivity.

■ ASSOCIATED CONTENT

SI Supporting Information

The Supporting Information is available free of charge at <https://pubs.acs.org/doi/10.1021/acs.jpcc.4c05807>.

Gas-phase spectra of 1,3-butadiene and 1-butene, calibration data of selected peak areas of gas-phase 1,3-butadiene and 1-butene versus pressure, Auger electron spectra of the Pd/Cu(111) surface before and after reaction, *p*- and *s*-polarized spectra and their difference for the product gas, examples of the peak fitting used to obtain selected peak areas to quantify amounts of 1,3-butadiene and 1-butene, and a table of 1,3-butadiene hydrogenation rates for different initial amounts of 1,3-butadiene and hydrogen (PDF)

■ AUTHOR INFORMATION

Corresponding Author

Michael Trenary — Department of Chemistry, University of Illinois Chicago, Chicago, Illinois 60607, United States;  orcid.org/0000-0003-1419-9252; Email: mtrenary@uic.edu

Author

Mohammad Rahat Hossain — Department of Chemistry, University of Illinois Chicago, Chicago, Illinois 60607, United States;  orcid.org/0000-0001-7947-7124

Complete contact information is available at:

<https://pubs.acs.org/10.1021/acs.jpcc.4c05807>

Notes

The authors declare no competing financial interest.

■ ACKNOWLEDGMENTS

This work was supported by a grant from the National Science Foundation, CHE-2102622.

■ REFERENCES

- (1) Selvakannan, P. R.; Hoang, L.; Kumar, V. V.; Dumbre, D.; Jampaiah, D.; Das, J.; Bhargava, S. K. Selective hydrogenation of 1,3-butadiene to 1-butene: Review on catalysts, selectivity, kinetics and reaction mechanism. In *Catalysis for Clean Energy and Environmental Stability- Petrochemicals and Refining Processes*, Pant, K. K.; Gupta, S. K.; Ahmad, E., Eds.; Vol. 2; Springer Nature: Switzerland, 2021; pp 205–228.
- (2) Aguilar-Tapia, A.; Delannoy, L.; Louis, C.; Han, C. W.; Ortalan, V.; Zanella, R. Selective hydrogenation of 1,3-butadiene over bimetallic Au-Ni/TiO₂ catalysts prepared by deposition-precipitation with urea. *J. Catal.* **2016**, *344*, 515–523.

(3) Lozano, L.; Brito, J. L.; Olivera, C.; Guerra, J.; Curbelo, S. Influence of toluene on the catalytic activity of NiPdCe catalyst for selective hydrogenation of 1,3-butadiene. *Fuel* **2013**, *110*, 76–82.

(4) Darby, M. T.; Stamatakis, M.; Michaelides, A.; Sykes, E. C. H. Lonely atoms with special gifts: breaking linear scaling relationships in heterogeneous catalysis with single-atom alloys. *J. Phys. Chem. Lett.* **2018**, *9* (18), 5636–5646.

(5) Lucci, F. R.; Liu, J.; Marcinkowski, M. D.; Yang, M.; Allard, L. F.; Flytzani-Stephanopoulos, M.; Sykes, E. C. H. Selective hydrogenation of 1,3-butadiene on platinum–copper alloys at the single-atom limit. *Nat. Commun.* **2015**, *6* (1), 8550–8550.

(6) Pradier, C.-M.; Margot, E.; Berthier, Y.; Oudar, J. Hydrogenation of 1,3-butadiene on Pt(111): Comparison with results on Pt(110) and Pt(100). *Appl. Catal.* **1988**, *43* (1), 177–192.

(7) Tourillon, G.; Cassuto, A.; Jugnet, Y.; Massardier, J.; Bertolini, J. Buta-1,3-diene and but-1-ene chemisorption on Pt(111), Pd(111), Pd(110) and Pd₅₀Cu₅₀(111) as studied by UPS, NEXAFS and HREELS in relation to catalysis. *J. Chem. Soc., Faraday Trans.* **1996**, *92* (23), 4835–4841.

(8) Ouchaib, T. Competitive hydrogenation of butadiene and butene on palladium and platinum catalysts. *J. Catal.* **1989**, *119* (2), 517–520.

(9) Massardier, J.; Bertolini, J.; Ruiz, P.; Delichere, P. Platinum single crystals: the effect of surface structure and the influence of K and Na on the activity and the selectivity for 1,3-butadiene hydrogenation. *J. Catal.* **1988**, *112* (1), 21–33.

(10) Lianos, L.; Debauge, Y.; Massardier, J.; Jugnet, Y.; Bertolini, J. 1,3-butadiene hydrogenation on Pd₅₀Cu₅₀ single crystals. *Catal. Lett.* **1997**, *44*, 211–216.

(11) Cooper, A.; Bachiller-Baeza, B.; Anderson, J.; Rodríguez-Ramos, I.; Guerrero-Ruiz, A. Design of surface sites for the selective hydrogenation of 1,3-butadiene on Pd nanoparticles: Cu bimetallic formation and sulfur poisoning. *Catal. Sci. Technol.* **2014**, *4* (5), 1446–1455.

(12) Kruppe, C. M.; Krooswyk, J. D.; Trenary, M. Polarization-dependent infrared spectroscopy of adsorbed carbon monoxide to probe the surface of a Pd/Cu(111) single-atom alloy. *J. Phys. Chem. C* **2017**, *121* (17), 9361–9369.

(13) Marcinkowski, M. D.; Jewell, A. D.; Stamatakis, M.; Boucher, M. B.; Lewis, E. A.; Murphy, C. J.; Kyriakou, G.; Sykes, E. C. H. Controlling a spillover pathway with the molecular cork effect. *Nat. Mater.* **2013**, *12* (6), 523–528.

(14) Kruppe, C. M.; Krooswyk, J. D.; Trenary, M. Selective hydrogenation of acetylene to ethylene in the presence of a carbonaceous surface layer on a Pd/Cu(111) single-atom alloy. *ACS Catal.* **2017**, *7* (12), 8042–8049.

(15) Abdel-Rahman, M. K.; Trenary, M. Propyne hydrogenation over a Pd/Cu(111) single-atom alloy studied using ambient pressure infrared spectroscopy. *ACS Catal.* **2020**, *10* (17), 9716–9724.

(16) Krooswyk, J. D.; Waluyo, I.; Trenary, M. Simultaneous monitoring of surface and gas phase species during hydrogenation of acetylene over Pt(111) by polarization-dependent infrared spectroscopy. *ACS Catal.* **2015**, *5* (8), 4725–4733.

(17) Islam, A.; Molina, D. L.; Trenary, M. Adsorption of acrolein and its hydrogenation products on Cu(111). *Phys. Chem. Chem. Phys.* **2022**, *24* (39), 24383–24393.

(18) Islam, A.; Abdel-Rahman, M. K.; Trenary, M. Heat of adsorption of propyne on Cu(111) from isotherms measured by reflection absorption infrared spectroscopy. *J. Phys. Chem. C* **2021**, *125* (34), 18786–18791.

(19) NIST Mass Spectrometry Data Center, W. E. W., director *Mass Spectra*; National Institute of Standards and Technology, 2024.

(20) Wiberg, K. B.; Rosenberg, R. E. Butadiene. 1. A normal coordinate analysis and infrared intensities. Structure of the second rotamer. *J. Am. Chem. Soc.* **1990**, *112* (4), 1509–1519.

(21) De Maré, G. R.; Panchenko, Y. N.; Vander Auwera, J. Structure of the high-energy conformer of 1,3-butadiene. *J. Phys. Chem. A* **1997**, *101* (22), 3998–4004.

(22) NIST Mass Spectrometry Data Center, W. E. W., director *Infrared Spectra*; National Institute of Standards and Technology, 2024.

(23) Kyriakou, G.; Boucher, M. B.; Jewell, A. D.; Lewis, E. A.; Lawton, T. J.; Baber, A. E.; Tierney, H. L.; Flytzani-Stephanopoulos, M.; Sykes, E. C. H. Isolated metal atom geometries as a strategy for selective heterogeneous hydrogenations. *Science* **2012**, *335* (6073), 1209–1212.

(24) Silvestre-Albero, J.; Rupprechter, G.; Freund, H.-J. Atmospheric pressure studies of selective 1,3-butadiene hydrogenation on Pd single crystals: effect of CO addition. *J. Catal.* **2005**, *235* (1), 52–59.

(25) Furlong, B. K.; Hightower, J. W.; Chan, T. Y.-L.; Sarkany, A.; Guczi, L. 1,3-Butadiene selective hydrogenation over Pd/alumina and CuPd/alumina catalysts. *Appl. Catal. A Gen.* **1994**, *117* (1), 41–51.

(26) Jugnet, Y.; Sedrati, R.; Bertolini, J. Selective hydrogenation of 1,3-butadiene on Pt₃Sn(111) alloys: comparison to Pt(111). *J. Catal.* **2005**, *229* (1), 252–258.

(27) Silvestre-Albero, J.; Borasio, M.; Rupprechter, G.; Freund, H.-J. Combined UHV and ambient pressure studies of 1,3-butadiene adsorption and reaction on Pd(111) by GC, IRAS and XPS. *Catal. Commun.* **2007**, *8* (3), 292–298.